17th World Conference on Earthquake Engineering, 17WCEE

Sendai, Japan - September 13th to 18th 2020

IMPACT OF EARTHQUAKE-INDUCED DEBRIS ON THE SEISMIC RESILIENCE OF ROAD NETWORKS

O.A. Sediek [1], S. El-Tawil [2], J.P. McCormick[3]

[1] *Ph.D. Student, Department of Civil and Environmental Engineering, University of Michigan, Ann Arbor, MI 48109, USA; email: osediek@umich.edu*

[2] *Professor, Department of Civil and Environmental Engineering, University of Michigan, Ann Arbor, MI 48109, USA; email: eltawil@umich.edu*

[2] *Associate Professor, Department of Civil and Environmental Engineering, University of Michigan, Ann Arbor, MI 48109, USA; email: jpmccorm@umich.edu*

Abstract

Collapse of buildings after seismic events can result in large amounts of debris that can block or reduce the capacity of adjacent sidewalks and roads. The debris zone can hinder emergency and evacuation operations, thereby adversely affecting the seismic resilience of a community. A model for the amount of debris generated due to a building collapse and its effect on road networks is developed using computational simulation. Eleven ground motions are applied to the studied building to study the variability in the collapse behavior of the building under different seismic events. The amount and extent of debris around the collapsed building is characterized to study the interaction between the collapsed buildings and surrounding roads. The presented results can be integrated in a regional simulation model or framework to simulate the interdependency between the debris generated from the collapsed buildings and the resilience of road networks.

Keywords: community resilience, disaster interdependencies, earthquake-induced debris, building collapse

1. Introduction

Destructive earthquakes produce large amounts of debris that can block or reduce the capacity of adjacent sidewalks and roads. There are numerous available examples in the literature for earthquakes that produced massive amounts of debris which hindered the recovery process of the community. One example is the 1995 Kobe earthquake which destroyed around 256,000 dwellings causing around 20 million tons of debris [1]. Early models are available in the literature for estimating the amount of seismic debris generated from different types of buildings based on the level of their post-earthquake damage [2]. However, none of these models provide detailed information about the extent (i.e. spread) of the debris around the buildings.

Seismic collapse of buildings is the major source of debris in the aftermath of seismic events. Available studies in this area [3-5] provide pre-assumed shapes of debris produced from collapsed buildings that do not necessarily correlate with real collapse scenarios. Further understanding of the behavior and resulting debris distribution associated with buildings that collapsed during an earthquake is hindered by difficulty in experimentally simulating complete collapse of a structure. Further, the high computational cost associated with high fidelity models limits their application. As an alternative, the finite element method (FEM) has been widely used for this purpose in the computational structural analysis field for decades. Many successful examples are available in the literature for modeling collapse behavior at the member [6] and system levels [7]. However, the high computational cost of those FE models required to simulate the collapse behavior of buildings has hindered their extension to simulate a large variety of collapse scenarios.

Emerging from the need to better understand the behavior and resulting debris pile associated with a collapsing building; a computational tool, the applied element method (AEM), was introduced a few decades ago based on discrete cracking [8]. AEM has been extensively developed over the past decade [9,10] to reliably simulate different collapse scenarios (e.g. seismic, blast, etc.). The idea behind the AEM is discretizing the structure into relatively small rigid elements connected together using a set of normal and shear springs that represents the constitutive relationship of the elements. All the deformations are evaluated at the springs instead of the elements as is done in FEM. Thus, AEM provides reliable modeling of the behavior of the

building from the elastic stage until the final collapse with considerably smaller computational time than FEM. It is reported by [11] that the computational time required for modeling the partial collapse of the Pyne Gould Corporation (PGC) Building after the 6.3 magnitude earthquake occurred in Christchurch, New Zealand using AEM on a personal computer is almost three times faster than using FEM on a high performance computer (HPC). Thus, this paper conducts computational simulations using AE models to study the collapse behavior of a prototype seismically designed reinforced concrete (RC) moment resisting frame structure subjected to different ground motion histories. The computational results are used to characterize the extent of debris around collapsed RC moment resisting frame buildings and study the effect of this debris field on adjacent road networks.

2. Applied Element Modeling

2.1 Prototype Building

The four-story space frame building outlined and designed in [12] is selected as a prototype building to characterize the debris field generated from the collapse of RC frame buildings. The building's plan is shown in Fig. 1. It consists of four RC special moment resisting frames in each direction which are assumed to resist all the seismic demands on the building. The building is designed for a general high seismic site in California (Design category D, soil class D, S_{ms} = 1.5g, and S_{m1} = 0.9g). The bay width is 9.10 m (30 ft), first story height is 4.57 m (15 ft), and the typical upper story height is 3.96 m (13 ft). The concrete compressive strength is 35 MPa (5 ksi) for both the beams and columns. The longitudinal rebar diameters commonly used in for detailing beams are 25 mm (#8) and 28 mm (#9) with a yield strength of 400 MPa (60 ksi). The design dead and live loads are 8 kN/m^2 (175 psf) and 2.4 kN/m^2 (50 psf), respectively. Further design details can be found in [12].

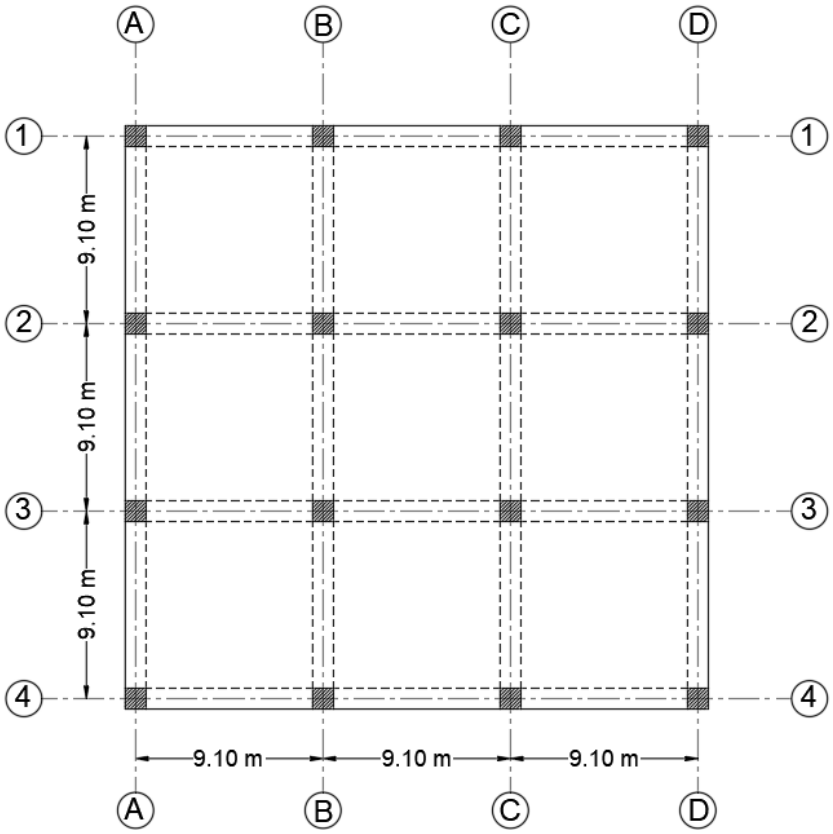

Fig. 1 – Plan of the prototype building

2.2 Modeling approach

Detailed applied element models of the prototype building, described earlier, are created using the AEM software Extreme Loading for Structures (ELS) [13] with a typical model shown in Fig. 2. The building model is discretized into relatively small cubical rigid elements connected together using a set of one normal and two orthogonal shear springs distributed along the element faces. The generation of the springs is done automatically in ELS. The element size is chosen based on a sensitivity study where the size of the elements is progressively halved until convergence. The Maekawa compression model [14] is used to simulate the compressive behavior of the concrete. The tensile behavior of the concrete is assumed to be linear until cracking where the tensile strength drops to zero and the residual stresses are redistributed in the next step. The shear behavior of the concrete is assumed to be linear until cracking where the shear stress drops by an amount based on the aggregate interlocking and friction at the crack surface.

The material model presented in [15] is used to model the behavior of the reinforcing steel bars which are modeled using different springs from the concrete springs. The reinforcement springs are placed at the location of the reinforcement bars where the rupture of the material takes place when the concrete springs between the considered faces reaches their separation strain. The exterior walls of the buildings are included in the AE model as shown in Fig. 2 to simulate the effect of exterior walls on the debris field of the building. The modeling approach for masonry walls described by [16] is implemented for the exterior walls since it has been validated against experimental data. The dimensions and properties of bricks and mortar are taken as given in [17] which is representative of walls in U.S. buildings. The building is assumed to be fully fixed at its base. Due to space limitations, the performed validation exercise is not presented herein. However, successful validations of the presented modeling approach can be found in [11,16]. Eleven ground motions are selected from the Far-Field record set in FEMA P695 [18] and scaled up until they induce total collapse of the prototype building. Table 1 lists the ground motion records employed in the presented study.

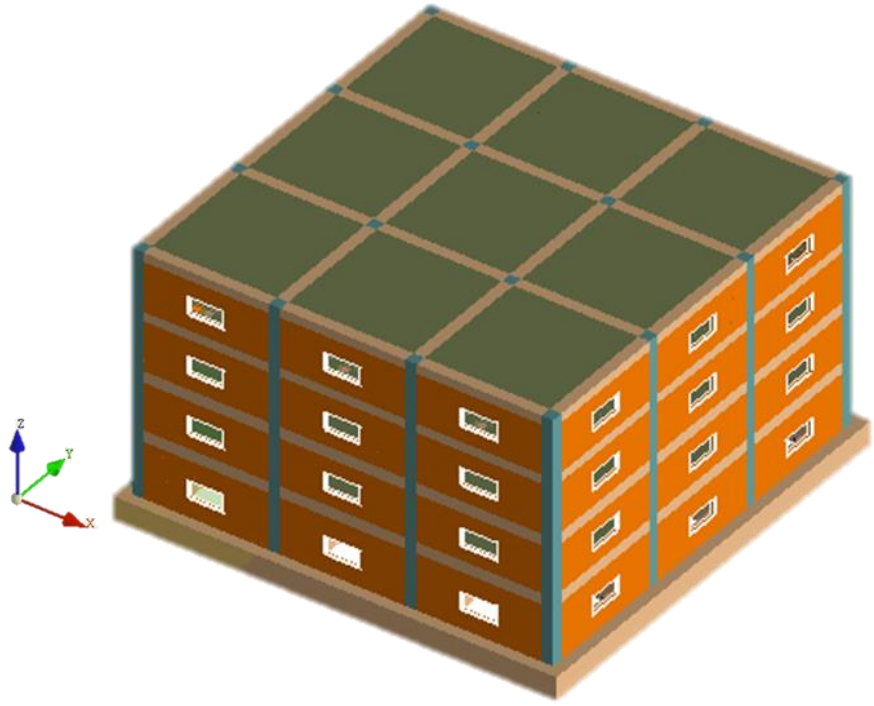

Fig. 2 – AE model of the prototype building

Table 1– Earthquake ground motion records employed in the collapse evaluation of the prototype building (from FEMA P695 [18])

No.	Event	Year	Magnitude (M_w)	Station	PGA (g) (Unscaled)
1	Northridge	1994	6.7	Beverly Hills-Mulhol	0.52
2	Northridge	1994	6.7	Canyon County-WLC	0.48
3	Düzce, Turkey	1999	7.1	Bolu	0.82
4	Hector Mine	1999	7.1	Hector	0.34
5	Imperial Valley	1979	6.5	Delta	0.35
6	Imperial Valley	1979	6.5	El Centro Array # 11	0.38
7	Kobe, Japan	1995	6.9	Nishi-Akashi	0.51
8	Kobe, Japan	1995	6.9	Shin-Osaka	0.24
9	Kocaeli, Turkey	1999	7.5	Düzce	0.36
10	Kocaeli, Turkey	1999	7.5	Arcelik	0.22
11	Landers	1992	7.3	Yermo Fire Station	0.24

3. Simulation Results

To facilitate the discussion of the results, the ground motions are labeled as GM_X where X is the number of the ground motion from the first column of Table 1. As shown in Fig. 3, four collapse modes are exhibited by the studied RC frame building based on the properties of the ground motion history, especially the relationship between the two horizontal components of the ground motion record. The first collapse mode is a pancake collapse type in the X-direction where most of the building debris is scattered in either the positive or negative direction of the X axis of the building. The second mode is similar to the first one except that most of the building debris is scattered in either the positive or negative direction of the Y axis of the building. Mode 3 and mode 4 are similar to each other where the building collapses in a skewed direction between its X and Y axis but with more debris skewed towards one of the two axes (X axis for mode 3 and Y axis for mode 4).

The amount of debris generated from the collapse of the prototype building is measured in the four directions outside the original envelope of the building as shown in Fig. 4. The variability of the results is considered probabilistically by fitting the results to a log-normal distribution as shown in Fig. 5. Two distributions are distinguished based on the collapse mode described earlier: the first distribution is for orthogonal collapse modes (i.e. mode 1 and mode 2) and is shown in Fig. 5 (a), while the second distribution is for skewed collapse modes (i.e. mode 3 and mode 4) and is shown in Fig. 5 (b). For the first distribution, the data is rearranged to consider four quantities: the maximum extent of debris, *Max* , (in X direction for mode 1 and in Y direction for mode 2), the debris extent in the same orthogonal direction as the maximum but on the opposite side of the building, *Min*, (i.e. the minimum or zero debris extent based on the collapse shapes shown in Fig. 3), and the other two debris extent dimensions, *Orth +ve* and *Orth -ve*, (i.e. in the other orthogonal direction). For the second distribution, the data is rearranged to consider four quantities: the two maximum debris extents, *max 1* and *max 2*, and the debris extents in the opposite side of the building from the two maximum extents, *Opp 1* and *Opp 2*.

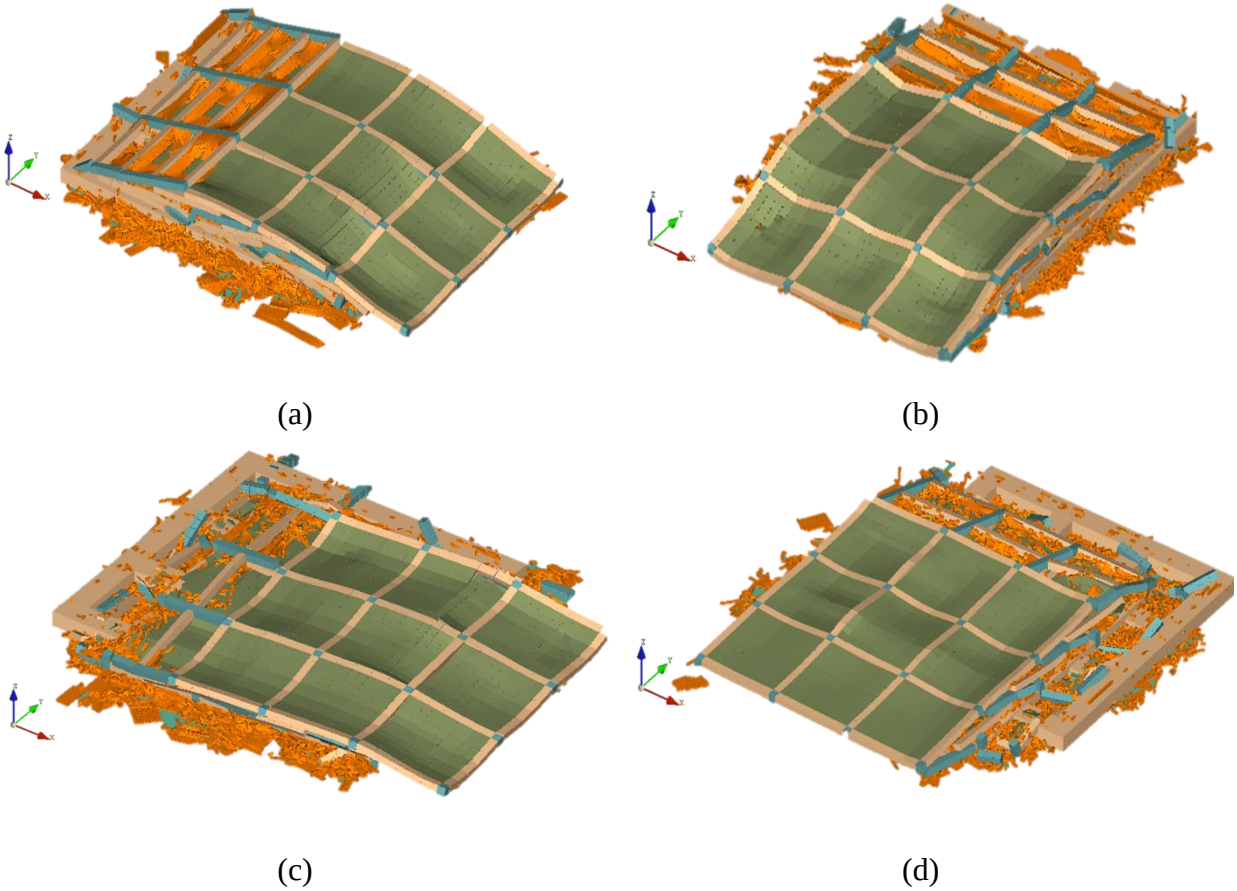

Fig. 3 – Final collapse shape for: (a) mode 1 (X-direction) under GM_11, (b) mode 2 (Y-direction) under GM_5, (c) mode 3 (skewed towards X) under GM_9, and (d) mode 4 (skewed towards Y) under GM_10

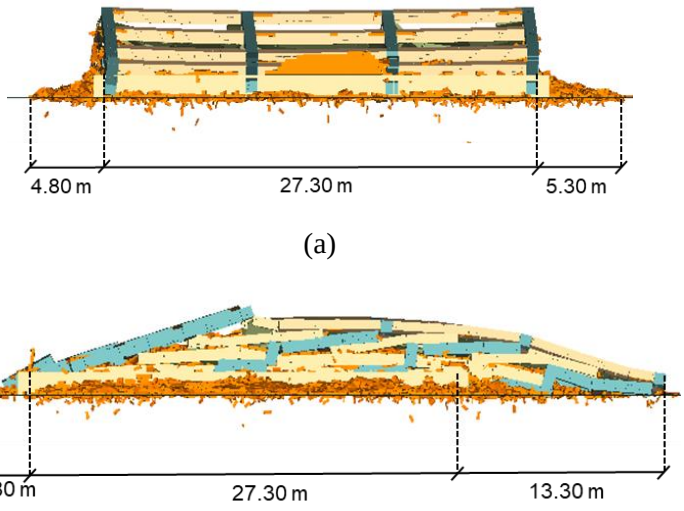

Fig. 4 – Measurement of the debris field under GM_7 in: (a) X direction, and (b) Y direction

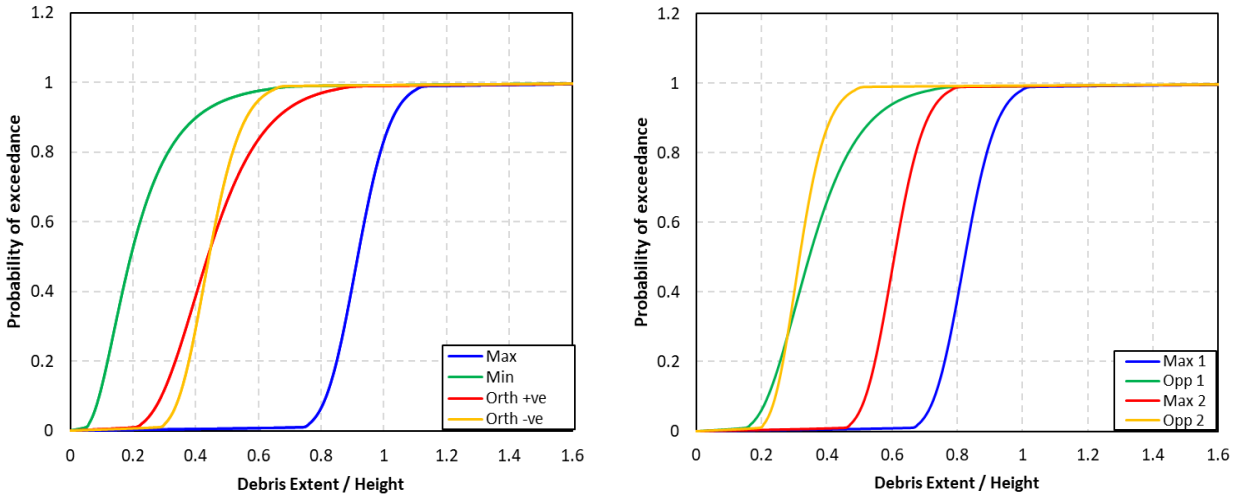

(a) (b)

Fig. 5 – Fitted log-normal cumulative density functions of the results for : (a) mode 1 and mode 2, and (b) mode 3 and mode 4

Fig. 6 shows the interaction between the studied prototype building and an adjacent typical 3-lane U.S. road before and after the seismic collapse of the building. As shown, the collapse of the four-story building almost blocked 50% of the road hindering the recovery and rescue processes in the aftermath of a seismic event. For taller buildings (i.e. more than four stories), the interaction between the debris and roadway will be even worse. Thus, further investigation is required for different building heights to thoroughly characterize the debris field resulting from the collapse of buildings due to an earthquake. This interaction can then be integrated into a multidisciplinary framework to better quantify the seismic resilience of road networks as well as the whole community.

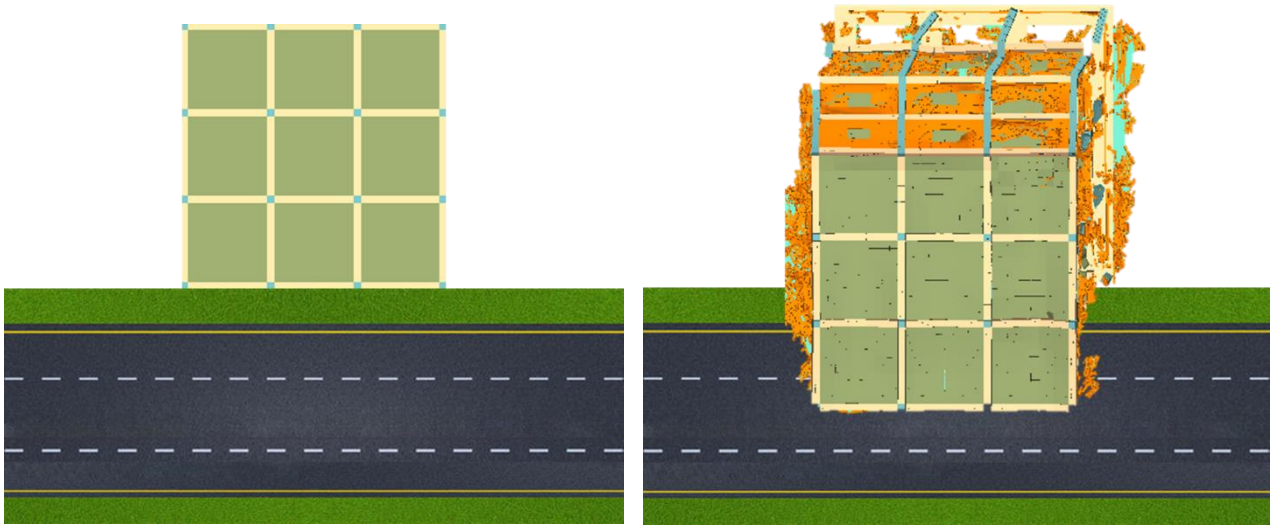

(a) (b)

Fig. 6 – Interaction between the prototype building and adjacent road: (a) before seismic collapse, and (b) after seismic collapse

4. Summary and Conclusions

The collapse behavior of a seismically designed prototype four-story RC moment resisting frame is studied using detailed applied element models. Eleven ground motions are selected from the Far-Field record set in FEMA P695 and scaled up until they induce total collapse of the building. Based on the analysis of the results, four modes of collapses can be distinguished: predominately in the X direction, predominately in the Y direction, skewed towards the X direction, and skewed towards the Y direction. The mode of collapse depends on the properties of the ground motion record, specifically the relationship between the two horizontal components of the ground motion. The extent of debris is measured in the four directions surrounding the envelope of the building to assess the interaction between the collapsed building and the adjacent roads. The results suggest that adjacent roads may be severely affected by the collapse of the studied building further hindering the recovery and rescue processes. The presented results can be integrated in a multidisciplinary framework to assess and quantify the seismic resilience of road networks as well as communities taking into consideration the interdependency between the structural system (i.e. the buildings) and the infrastructure system (i.e. roads).

5. Acknowledgements

This work was supported by the University of Michigan, University of Delaware and the US National Science Foundation (NSF) through grant ACI-1638186. Any opinions, findings, conclusions, and recommendations expressed in this paper are those of the authors and do not necessarily reflect the views of the sponsor.

6. References

[1] Tabata T, Onishi A, Saeki T, Tsai P (2019): Earthquake disaster waste management reviews: Prediction, treatment, recycling, and prevention. *International Journal of Disaster Risk Reduction*, **36**, 101-109.

[2] FEMA (2003): Earthquake loss estimation methodology: Technical manual. *National Institute of Building for the Federal Emergency Management Agency, Washington, DC.*

[3] Goretti A, Sarli V (2006): Road Network and Damaged Buildings in Urban Areas: Short and Long-term Interaction. *Bulletin of Earthquake Engineering*, **4**, 159–175

[4] Hirokawa N, Osaragi T (2016): Earthquake Disaster Simulation System: Integration of Models for Building Collapse, Road Blockage, and Fire Spread. *Journal of Disaster Research* **11**(2).

[5] Castro S, Poulos A, Herrera JC, de la Llera, JC (2019): Modeling the Impact of Earthquake-Induced Debris on Tsunami Evacuation Times of Coastal Cities. *Earthquake Spectra*, **35** (1), 137–158.

[6] Sediek OA, Wu TY, McCormick J, El-Tawil S, (2020): Collapse Behavior of HSS Columns Under Combined Axial and Lateral Loading. *Journal of Structural Engineering*, 10.1061/(ASCE)ST.1943-541X.0002637.

[7] Wu TY, El-Tawil S, McCormick, J (2018): Seismic Collapse Response of Steel Moment Frames with Deep Columns. *Journal of Structural Engineering*, **144** (9).

[8] Meguro K, Tagel-Din H. (2000): Applied element method for structural analysis: theory and application for linear materials. *Struct Eng/Earthquake Eng JSCE* **17** (1):21s–35s.

[9] Meguro K (2001): Applied element method: a new efficient tool for design of structure considering its failure behavior. *Institution of Industrial Science (IIS). Japan, September: The university of Tokyo*. p. 1–20.

[10] Meguro K, Tagel-Din H. (2001): Applied element simulation of RC structures under cyclic loading. *Journal of Structural Engineering*, **127**(11) 1295-1305

[11] Grunwald C, Khalil AA, Schaufelberger B, Ricciardi EM, Pellecchia C, Iuliis ED, Riedel W (2018): Reliability of collapse simulation - Comparing finite and applied element method at different levels. *Engineering Structures*, **176** (2018) 265-278

[12] Haselton, C (2006): Assessing Seismic Collapse Safety of Modern Reinforced Concrete Moment-Frame Buildings. *The Blume Earthquake Engineering Center*, Stanford University.

[13] Applied Science International, LLC, Extreme loading for structures theoretical manual; 2017.

[14] Maekawa K, Pimanmas, A, Okamura H (2003): Nonlinear Mechanics of Reinforced Concrete. *Spon Press: London, UK*.

[15] Menegotto M, Pinto P (1973): Method of analysis for cyclically loaded reinforced concrete plane frames including changes in geometry and non-elastic behavior of elements under combined normal force and bending. *In IABSE Symposium of Resistance and Ultimate Deformability of Structure*, Zurich, Switzerland.

[16] Domaneschi M, Cimellaro GP, Scutiero G (2019): A simplified method to assess generation of seismic debris for masonry structures. *Engineering Structures*, **186** (2019) 306-320

[17] Aref A, Dolatshahi AM (2013): A three-dimensional cyclic meso-scale numerical procedure for simulation of unreinforced masonry structures. *Computers and Structures*, **120** (2013) 9–23.

[18] FEMA. (2009): Quantification of building seismic performance factors. *Report No. FEMA-P695, Federal Emergency Management Agency*, Washington, D.C.

